

Radiating fluid spheres in the effective variables approximation

W. Barreto and B. Rodríguez

Grupo de Relatividad y Astrofísica Teórica,
Departamento de Física, Escuela de Ciencias, Núcleo de Sucre,
Universidad de Oriente, Cumaná, Venezuela

H. Martínez

Sección de Física, Unidad de Estudios Generales,
Universidad Nacional Experimental Politécnica Antonio José de Sucre,
Puerto Ordaz, Venezuela

November 2, 2018

Abstract

We study the evolution of spherically symmetric radiating fluid distributions using the effective variables method, implemented *ab initio* in Schwarzschild coordinates. To illustrate the procedure and to establish some comparison with the original method, we integrate numerically the set of equations at the surface for two different models. The first model is derived from the Schwarzschild interior solution. The second model is inspired in the Tolman VI solution.

1 INTRODUCTION

In 1980, Herrera, Jiménez and Ruggeri proposed a seminumerical method, hereafter referred to as the effective variables method (EVM), that can be used to obtain nonstatic models from static solutions. This method divides the spacetime in two spatial regions. The outer region is described by the Vaidya solution and the spacetime metric in the interior is obtained by solving the Einstein field equations. Further, proper boundary conditions are imposed in order to guarantee a smooth matching of both solutions. The EVM has been used extensively to study astrophysical scenarios in radiative coordinates [1, 2]. The method assumes that the called effective variables $\tilde{\rho}$ and \tilde{p} , which depend also on the time-like coordinate, have the same radial dependence as the corresponding static physical variables (energy density and pressure) obtained from a static interior solution of the Einstein equations. The rationale behind such an assumption is the fact that the effective variables reduce to their physical counterparts in the static limit. This approach can be justified by means of

the characteristic times for different processes which take place in the collapse scenario [3, 4, 5]. If the hydrostatic time scale, $\tau_{hydr.} \approx 1/\sqrt{G\rho}$, is much shorter than the Kelvin–Helmholtz time scale τ_{KH} , then in a first approximation the inertial terms in the equation of motion can be ignored. Consequently, it seems reasonable to assume, in this approximation, that the radial dependence of the physical variables is the same as in the static solution. However, a better approximation is obtained by assuming that the effective variables, not the physical ones, have the same radial dependence as the corresponding physical variables of the static situation [1].

If the EVM is truly general, an implementation in Schwarzschild coordinates could be more interesting for astrophysicists since these are the type of coordinates commonly used by them; this is successfully accomplished in this paper. The idea that we can always construct dynamical solutions from static ones seems a general method. Besides, as we will show, the EVM in Schwarzschild coordinates introduces higher dynamic corrections, by means of the velocity respect to a minkowskian observer, than those obtained in the Bondi coordinates treatment.

In this paper we model two simple but physically meaningful scenarios. The first is obtained from a static solution for an incompressible fluid. Once the sphere departs from static equilibrium by the emission of energy, it slowly recovers the initial state (staticity), unless some energy can be reabsorbed at the surface to reach a constant radius in short time. In fact we show that even in Bondi coordinates the same result holds if staticity at the surface is enforced. The second model corresponds to a highly compressed gas of fermions, Tolman’s solution VI [6], and leads us to an exploding sphere as has been reported [1, 7]. Additionally, these seminumerical models could serve as useful test beds for the numerical relativity methods being developed to match Cauchy and characteristic codes [8]–[15]

The paper is organized as follows. In section 2 we write the field equations, for the inner region, in Schwarzschild coordinates. Describing the exterior space–time by means of the Vaidya metric, in section 3, we treat the matching conditions and write the equations at the boundary of the distribution of matter. In the section 4 we show our two models; finally we conclude in section 5.

2 FIELD EQUATIONS

To write the Einstein field equations, inside the distribution of matter, we use the line element in Schwarzschild coordinates

$$ds^2 = e^\nu dt^2 - e^\lambda dr^2 - r^2 (d\theta^2 + \sin^2\theta d\phi^2), \quad (1)$$

where $\nu = \nu(t, r)$ and $\lambda = \lambda(t, r)$, with $(t, r, \theta, \phi) \equiv (0, 1, 2, 3)$.

Physical input is obtained by introducing Minkowski coordinates (τ, x, y, z) by [16]

$$d\tau = e^{\nu/2} dt, \quad dx = e^{\lambda/2} dr, \quad dy = r d\theta, \quad dz = r \sin\theta d\phi. \quad (2)$$

In these expressions ν and λ are constants, because they only have local values.

Next we assume that, for an observer moving relative to these coordinates with velocity ω in the radial (x) direction, the space is filled with a fluid of density ρ , pressure p , and unpolarized radiation of energy density $\hat{\epsilon}$. For this comoving observer, the covariant energy tensor in Minkowski coordinates is

$$\begin{pmatrix} \rho + \hat{\epsilon} & -\hat{\epsilon} & 0 & 0 \\ -\hat{\epsilon} & p + \hat{\epsilon} & 0 & 0 \\ 0 & 0 & p & 0 \\ 0 & 0 & 0 & p \end{pmatrix}. \quad (3)$$

Note that from (2) the velocity of matter in the Schwarzschild coordinates is

$$\frac{dr}{dt} = \omega e^{(\nu-\lambda)/2}. \quad (4)$$

Now, by means of a Lorentz boost and defining $\epsilon \equiv \hat{\epsilon}(1+\omega)/(1-\omega)$ we write the field equations in relativistic units ($G = c = 1$) as follows:

$$\frac{\rho + p\omega^2}{1 - \omega^2} + \epsilon = \frac{1}{8\pi r} \left[\frac{1}{r} - e^{-\lambda} \left(\frac{1}{r} - \lambda_{,r} \right) \right], \quad (5)$$

$$\frac{p + \rho\omega^2}{1 - \omega^2} + \epsilon = \frac{1}{8\pi r} \left[e^{-\lambda} \left(\frac{1}{r} + \nu_{,r} \right) - \frac{1}{r} \right], \quad (6)$$

$$p = \frac{1}{32\pi} \left\{ e^{-\lambda} [2\nu_{,rr} + \nu_{,r}^2 - \lambda_{,r}\nu_{,r} + \frac{2}{r}(\nu_{,r} - \lambda_{,r})] - e^{-\nu} [2\lambda_{,tt} + \lambda_{,t}(\lambda_{,t} - \nu_{,t})] \right\}, \quad (7)$$

$$(\rho + p) \frac{\omega}{1 - \omega^2} + \epsilon = -\frac{\lambda_{,t}}{8\pi r} e^{-\frac{1}{2}(\nu+\lambda)}, \quad (8)$$

where the comma subscript represents partial differentiation with respect to the indicated coordinate.

We have four field equations for four physical variables (ρ , p , ϵ and ω) and two geometrical variables (ν and λ). Obviously, additional information is required to handle the problem consistently. First, however, we discuss the matching with the exterior solution and the surface equations that govern the dynamics.

3 MATCHING CONDITIONS AND SURFACE EQUATIONS

We describe the exterior space-time by the Vaidya metric

$$ds^2 = \left(1 - \frac{2\mathcal{M}(u)}{R} \right) du^2 + 2du dR - R^2 (d\theta^2 + \sin^2 \theta d\phi^2), \quad (9)$$

where u is a time-like coordinate so that $u = \text{constant}$ represents, asymptotically, null cones open to the future and R is a null coordinate ($g_{RR} = 0$).

The exterior and interior solutions are separated by the surface $r = a(t)$. To match both regions on this surface we require the Darmois matching conditions. Thus, demanding the continuity of the first fundamental form, we obtain

$$e^{-\lambda_a} = 1 - \frac{2\mathcal{M}}{R_a} \quad (10)$$

and

$$\nu_a = -\lambda_a. \quad (11)$$

From now on, the subscript a indicates that the quantity is evaluated at the surface. Matching conditions are usually obtained from the continuity of the first and second fundamental forms. Here, however, we will use the continuity of the independent components of the energy-momentum flow instead of the second fundamental form, which have been shown to be equivalent [17] but it is simpler to apply in the present case. This last condition guarantees absence of singular behaviors on the surface. It is easy to check that

$$p_a = 0, \quad (12)$$

which expresses the continuity of the radial pressure.

To write the surface equations we introduce the mass function m by means of

$$e^{-\lambda(r,t)} = 1 - 2m(r,t)/r. \quad (13)$$

Substituting (13) into (5) and (8) we obtain, after some rearrangements,

$$\frac{dm}{dt} = -4\pi r^2 \left[\frac{dr}{dt} p + \epsilon(1 - \omega) \left(1 - \frac{2m}{r}\right)^{1/2} e^{\nu/2} \right]. \quad (14)$$

This equation shows the energetics across the moving boundary of the fluid sphere. Evaluating (14) at the surface and using the boundary condition (12), the energy loss is given by

$$\dot{m}_a = -4\pi a^2 \epsilon_a (1 - 2m_a/a)(1 - \omega_a). \quad (15)$$

Hereafter, a dot over any variable indicates d/dt . The evolution of the boundary is governed by equation (4) evaluated at the surface

$$\dot{a} = (1 - 2m_a/a)\omega_a. \quad (16)$$

Scaling the total mass m_a , the radius a and the time-like coordinate by the initial mass $m_a(t=0) \equiv m_a(0)$,

$$A \equiv a/m_a(0), \quad M \equiv m_a/m_a(0), \quad t/m_a(0) \rightarrow t,$$

it is convenient to define

$$F \equiv 1 - 2M/A, \quad (17)$$

$$\Omega \equiv \omega_a. \quad (18)$$

Also we define the luminosity as seen by a comoving observer as [3]

$$\hat{E} \equiv (4\pi r^2 \dot{\epsilon})_{r=a}, \quad (19)$$

and the luminosity perceived by an observer at rest at infinity as

$$L \equiv -\dot{M} = F\hat{E}(1 + \Omega). \quad (20)$$

The function F is related to the boundary redshift z_a by

$$1 + z_a = \frac{\nu_{em}}{\nu_{rec}} = F^{-1/2}. \quad (21)$$

Thus the luminosity as measured by a noncomoving observer located on the surface is

$$E = L(1 + z_a)^2 = -\frac{\dot{M}}{F} = \hat{E}(1 + \Omega), \quad (22)$$

where the term $(1 + \Omega)$ accounts for the boundary Doppler shift. With these definitions the surface equations can be written as

$$\dot{A} = F\Omega, \quad (23)$$

$$\dot{F} = \frac{(1 - F)\dot{A} + 2L}{A}. \quad (24)$$

Equations (23) and (24) are general within spherical symmetry. We need a third surface equation to specify the dynamics completely for any set of initial conditions and a given luminosity profile $L(t)$. For this purpose we can use the conservation equation $T_{1;\mu}^\mu = 0$ evaluated at the surface. After straightforward manipulations the condition $T_{1;\mu}^\mu = 0$ results in

$$\begin{aligned} \tilde{p}_{,r} + \frac{(\tilde{\rho} + \tilde{p})(4\pi r^3 \tilde{p} + m)}{r(r - 2m)} = \\ \frac{e^{-\nu}}{4\pi r(r - 2m)} \left(m_{,tt} + \frac{3m_{,t}^2}{r - 2m} - \frac{m_{,t}\nu_{,t}}{2} \right) + \frac{2}{r}(p - \tilde{p}), \end{aligned} \quad (25)$$

where the effective variables are defined by

$$\tilde{\rho} \equiv \frac{\rho + p\omega^2}{1 - \omega^2} + \epsilon \quad (26)$$

and

$$\tilde{p} \equiv \frac{p + \rho\omega^2}{1 - \omega^2} + \epsilon. \quad (27)$$

These effective variables are essentially the same as have been defined by Herrera and collaborators, but now the velocity ω introduces a higher dynamics correction (quadratic). This fact could be of interest to investigate its effect on dissipative processes (like heat flow and viscosity).

Equation (25) is the generalization of the Tolman–Oppenheimer–Volkov equation for hydrostatic support in nonstatic radiative situations. Our equation leads at the surface to a differential equation for Ω if we specify in some way the geometrical variables.

4 MODELING

From (5), (6) and (13), easily we obtain

$$m = \int_0^r 4\pi r^2 \tilde{\rho} dr, \quad (28)$$

$$\nu = \nu_a + \int_a^r \frac{2(4\pi r^3 \tilde{p} + m)}{r(r-2m)} dr. \quad (29)$$

Thus, m and ν are expressed in terms of $\tilde{\rho}$ and \tilde{p} in the nonstatic case in the same way they are in terms of ρ and p in the static case. These considerations suggest the application of the EVM which until now has been exclusively used in Bondi coordinates [1, 2]; that is, we assume that the r dependence on $\tilde{\rho}$ and \tilde{p} is the same as on the ρ_{static} and p_{static} .

To illustrate the procedure, in what follows we model two simple scenarios which correspond to an incompressible fluid and to a highly compressed gas of fermions.

4.1 Schwarzschild-like model

Consider the well known Schwarzschild interior solution, where the density satisfies $\rho = constant$. Thus, in the EVM we take the effective density as

$$\tilde{\rho} = f(t), \quad (30)$$

where f is an arbitrary function of t . Now, with $\rho = constant$ we can integrate equation (25) in the static case and obtain the expression for p which leads us to

$$\frac{\tilde{p} + \frac{1}{3}\tilde{\rho}}{\tilde{p} + \tilde{\rho}} = \left(1 - \frac{8\pi}{3}\tilde{\rho}r^2\right)^{1/2} k(t), \quad (31)$$

where k is a function of t to be defined from the boundary condition (12), which now reads, in terms of the effective variables, as

$$\tilde{p}_a = \tilde{\rho}_a \Omega^2 + \epsilon_a (1 - \Omega^2). \quad (32)$$

Thus, (31) and (32) give

$$\tilde{\rho} = \frac{3(1-F)}{8\pi a^2}, \quad (33)$$

$$\tilde{p} = \frac{\tilde{\rho}}{3} \left\{ \frac{\chi_S \sqrt{F} - 3\psi_S \xi}{\psi_S \xi - \chi_S \sqrt{F}} \right\}, \quad (34)$$

with

$$\xi = [1 - (1-F)(r/a)^2]^{1/2}$$

and

$$\chi_S = 3(\Omega^2 + 1)(1-F) + 2E(1 + \Omega),$$

$$\psi_S = (3\Omega^2 + 1)(1 - F) + 2E(1 + \Omega).$$

Using (28) and (29) it is easy to obtain expressions for m and ν :

$$m = m_a(r/a)^3, \quad (35)$$

$$e^\nu = \left\{ \frac{\chi_S \sqrt{F} - \psi_S \xi}{2(1 - F)} \right\}^2. \quad (36)$$

In order to write down explicitly the surface equations for this example, it is interesting to note that the left side of (25) is zero for any value of $f(t)$. Next, evaluating (25) at the surface, we obtain

$$\begin{aligned} \dot{\Omega} = \frac{2}{3F(1 - F)} & \left\{ \left[\frac{3}{AF} \left(FE + \frac{3}{2}(1 - F)\dot{A} \right) \right. \right. \\ & + \left. \left(\dot{F} - \frac{\dot{A}\psi_S}{A} \right) \right] \left(FE + \frac{3}{2}(1 - F)\dot{A} \right) \\ & + \frac{6FE\dot{A}}{A} + \frac{6(1 - F)\dot{A}^2}{A} - \dot{F}E - F\dot{E} \\ & \left. - \frac{3}{2}(1 - F)\dot{F}\Omega - \frac{F^2}{A}[\psi_S - (1 - F)] \right\}. \quad (37) \end{aligned}$$

This last equation, together with (23) and (24), constitute the differential system for the surface in this example. It is necessary to specify one function of t and the initial data. To compare with Ref. [1] we choose L to be a gaussian and radiating away 1/10 of the initial mass. Therefore, the system can be numerically integrated for the following initial conditions (among others):

$$A(0) = 5.0, \quad F(0) = 0.6, \quad \Omega = 0.0.$$

The integration was done up to some t with good behavior in the physical variables.

Feeding back the numerical values of A , F and Ω (and their derivatives) in (35) and (36) we obtain m and ν (and their partial derivatives) for any value of r . Thus, functions ρ , p , dr/dt and ϵ can be monitored for any piece of the material, via field equations. We calculated them for the values $r/a = 0.2, 0.4, 0.6, 0.8$ and 1.0 . It is interesting to observe that once the sphere departs from static equilibrium by means of an emission of energy, it will not recover a constant radius at all, at least within the integrated interval of time. This behavior is not evident in Bondi coordinates, as we show below. Figure 1 shows the evolution of the radius A in a logarithmic scale. Figure 2 displays the profiles of the physical variables versus the time-like coordinate for the different comoving regions.

In order to explore the slow recovery of staticity at the surface we force it to return to rest quickly after the emission of energy; we prescribe its evolution

instead of giving the luminosity L . For such a prescription the surface equations change; now we obtain the luminosity profile from a differential equation. We choose a radius evolving as

$$A(t) = \frac{(A_i - A_f)(e^{-t_d/\sigma} + 1)}{e^{(t-t_d)/\sigma} + 1} + A_f,$$

where A_i is the initial radius, A_f the final radius, t_d the decay time and σ is the decay rate. Figure 3 shows the luminosity profile and the prescribed radius. Observe that it is necessary to absorb some quantity of energy (less than the total emitted) to reach a final constant radius. We confirmed the same behavior in Bondi coordinates. It is interesting to note that in Ref. [1] the interior profiles of the flux radiation (for the Schwarzschild type model) have the same qualitative behavior as we show in Figure 3: It is clear the absorption of energy.

4.2 Tolman VI-like model

In this subsection we discuss the model obtained from Tolman's solution VI [1], [6]. Let us take

$$\tilde{\rho} = \frac{3g}{r^2}, \quad (38)$$

$$\tilde{p} = \frac{g}{r^2} \left\{ \frac{1 - 9Dr}{1 - Dr} \right\}, \quad (39)$$

where g and D are functions of t , which can be determined using (32). Thus,

$$\tilde{\rho} = \frac{3(1 - F)}{24\pi r^2}, \quad (40)$$

$$\tilde{p} = \frac{(1 - F)}{24\pi r^2} \left\{ \frac{\psi_T - 9\chi_T(r/a)}{\psi_T - \chi_T(r/a)} \right\}, \quad (41)$$

where

$$\chi_T = (3\Omega^2 - 1)(1 - F) + 6E(1 + \Omega),$$

$$\psi_T = 3(\Omega^2 - 3)(1 - F) + 6E(1 + \Omega).$$

Using (28) and (29) we obtain

$$m = m_a r/a, \quad (42)$$

$$e^\nu = F \left\{ \left(\frac{\psi_T - \chi_T(r/a)}{\psi_T - \chi_T} \right)^2 (r/a) \right\}^{4(1-F)/3F}. \quad (43)$$

In this model, the LHS of (25) results in

$$\begin{aligned} \tilde{R}(t) = & \frac{(1 - F)}{12\pi a^3 (\psi_T - \chi_T)} \left\{ \frac{(\psi_T - 9\chi_T)\chi_T}{2(\psi_T - \chi_T)} - \psi_T + \frac{9\chi_T}{2} \right\} + \\ & \frac{1}{16\pi a^3 F} [(1 - F)(1 + \Omega^2) + 2E(1 + \Omega)]^2, \end{aligned} \quad (44)$$

which lets us write the third equation at the surface as

$$\dot{\Omega} = \frac{2}{F(1-F)} \left\{ \frac{\dot{F}^2 A}{4F} + \dot{F} \dot{A} + \frac{\dot{F} A}{4F} \left\{ \dot{F} - \frac{\dot{A}}{A} [(1-F)(\Omega^2 + 1) + 2E(1 + \Omega)] \right\} - \left\{ \dot{E} F + 4\pi A^2 F^2 \dot{R} + \frac{F^2}{A} [(1-F)\Omega^2 + 2E(1 + \Omega)] \right\} \right\}. \quad (45)$$

Again the system can be numerically integrated for a reasonable set of initial conditions (with L being a gaussian as in the Schwarzschild-like model, radiating away 1/100 of the initial mass), as for example,

$$A(0) = 6.67, \quad F(0) = 0.70, \quad \Omega = -0.17.$$

Figure 4 shows the evolution of the radius of the sphere. Initially the fluid sphere collapses, but later it bounces. Figure 5 gives the evolution of the matter variables for different regions. Note, for the matter velocity profiles, that some inner zones continue contracting after the bounce of the outermost ones.

5 CONCLUDING REMARKS

We have sought the dependence of the EVM upon the Bondi coordinates. The idea that we can always construct dynamical solutions from static ones seems a general method. In this paper we accomplish successfully such a construction, at least, for the Schwarzschild coordinates. Some research is in progress for more realistic luminosity profiles and dissipative transport mechanisms, considering extended thermodynamics under the time relaxation approximation. We considered in this paper two simple and idealized models, not deprived of physical meaning at all. We may hope that they contain some of the essential features of gravitational collapse inasmuch as we have fed the models with some observational data (initial velocity and total mass radiated.) Also, we can hope that our toy models could serve as test beds for the numerical relativity methods and codes.

Acknowledgements

We benefited from research support by the Consejo de Investigación under Grant CI-5-1001-0774/96 of the Universidad de Oriente. We thank the Postgrado en Física program of the Universidad de Oriente for the support received and to Luis Lehner for his valuable comments.

References

- [1] Herrera, L., Jiménez, J. and Ruggeri, G.: 1980, *Phys. Rev. D* **22**, 2305.
- [2] Herrera, L. and Núñez, L.: 1990, *Fund. Cosmic Phys.* **14**, 235.
- [3] Martínez, J.: 1996, *Phys. Rev. D* **53**, 6921.
- [4] Kippenhan, R., and Weigert, A.: 1990, *Stellar Structure and Evolution* (Berlin: Springer-Verlag).
- [5] Burrows, A. and Lattimer, J. M.: 1986, *Astrophys. J.* **307**, 178.
- [6] Tolman, R.: 1939, *Phys. Rev.* **55**, 364.
- [7] Barreto, W.: 1993, *Astrophys. and Space Sc.* **201**, 191.
- [8] Bishop, N. T.: 1992, In *Approaches to Numerical Relativity*, edited by d’Inverno, R. A. (Cambridge University Press, Cambridge, England) pp. 20–33.
- [9] Bishop, N. T.: 1993, *Class Quantum Grav.* **10**, 333.
- [10] Bishop, N. T., Gómez, R., Holvorcem, P. R., Matzner, R. A., Papadopoulos, P. and Winicour, J.: 1996, *Phys. Rev. Lett.* **76**, 4303.
- [11] Bishop, N. T., Gómez, R., Lehner, L. and Winicour, J.: 1996, *Phys. Rev. D* **54**, 6153.
- [12] Clarke, C. J. S., d’Inverno, R. A. and Vickers, J.: 1995, *Phys. Rev. D* **52**, 6863.
- [13] d’Inverno, R. A. and Vickers, J. A.: 1996, *ibid.* **54**, 4919.
- [14] d’Inverno, R. A. and Vickers, J. A.: 1997, *ibid.* **56**, 772.
- [15] Dubal, M. R., d’Inverno, R. A. and Clarke, C. J. S.: 1995, *ibid.* **52**, 6868.
- [16] Bondi, H.: 1964, *Proc. Roy. Soc. London*, **A281**, 39.
- [17] Herrera, L. and Di Prisco, A.: 1997, *Phys. Rev. D* **55**, 2044.

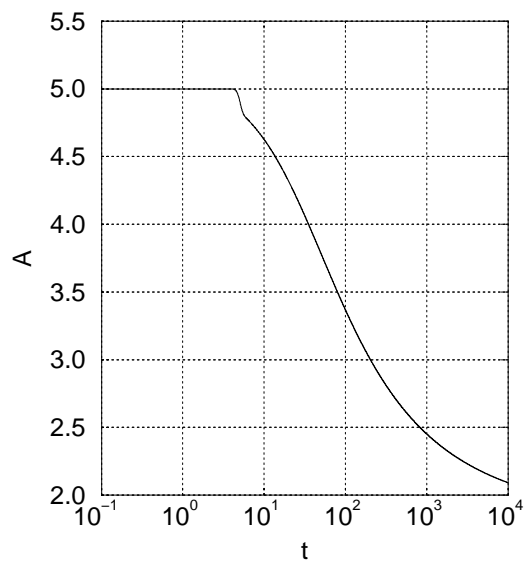


Figure 1: Evolution of the radius for the Schwarzschild type model.

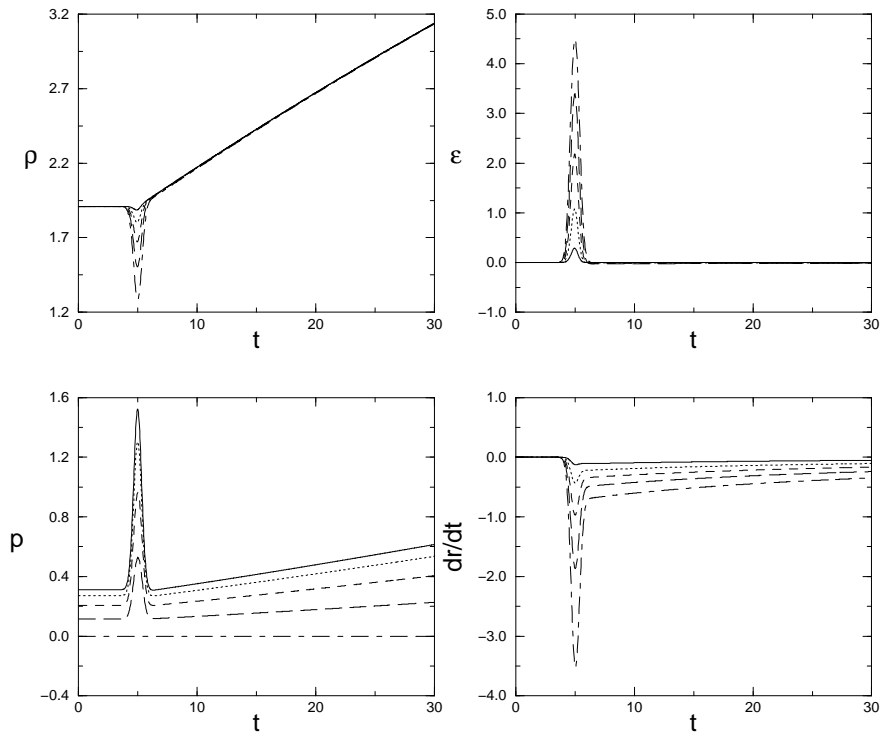


Figure 2: Density (multiplied by 10^3), energy density flux (multiplied by 10^4), pressure (multiplied by 10^3) and matter velocity (multiplied by 10) for the Schwarzschild type model as a function of the time-like coordinate and different pieces of the material: 0.2 (solid line); 0.4 (dotted line); 0.6 (small-dashed line); 0.8 (dashed line); 1.0 (dot-dashed line.)

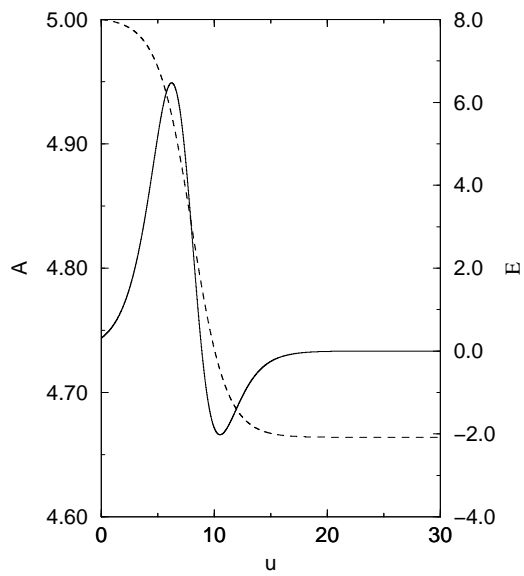
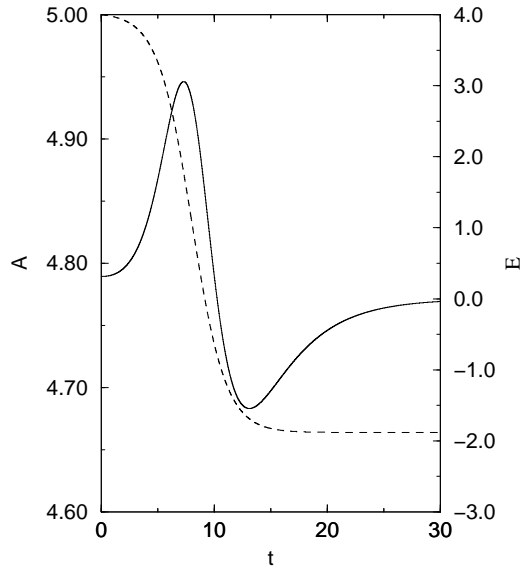


Figure 3: Evolution of the enforced radius A (dashed line) and the resulting luminosity E (solid line multiplied by 10^2) for the Schwarzschild type model in Schwarzschild and Bondi coordinates.

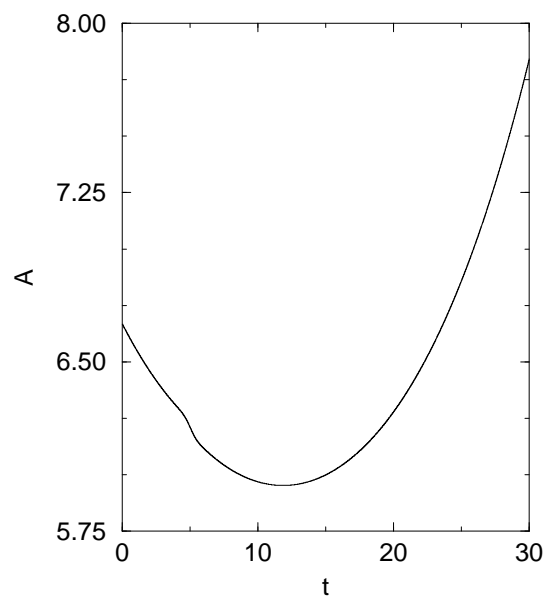


Figure 4: Evolution of the radius for the Tolman VI type model.

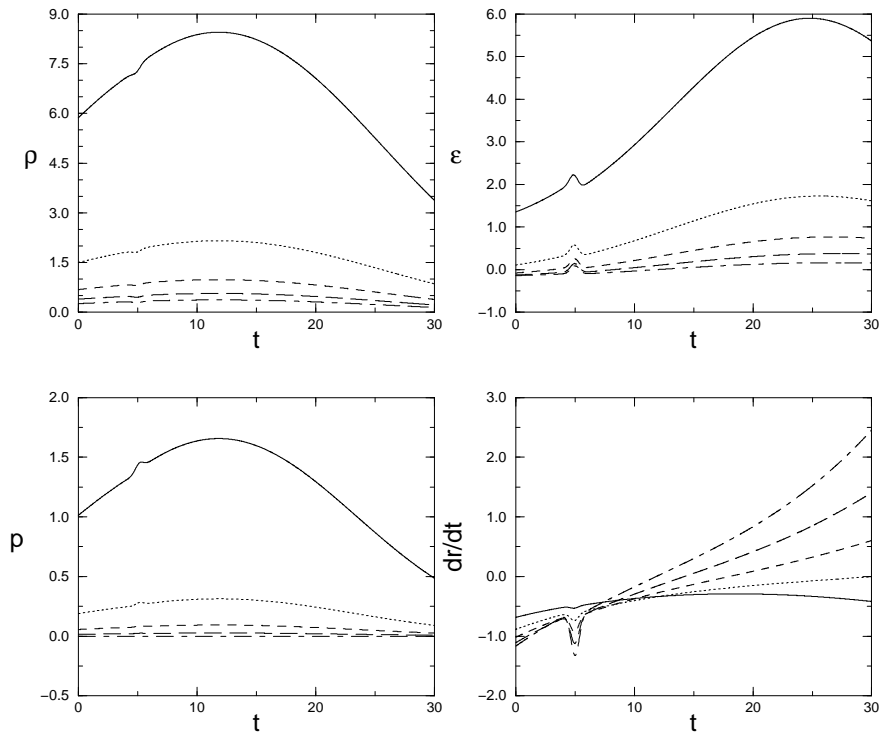


Figure 5: Density (multiplied by 10^3), energy density flux (multiplied by 10^4), pressure (multiplied by 10^3) and matter velocity (multiplied by 10) for the Tolman VI type model as a function of the time-like coordinate and different pieces of the material: $r/a = 0.2$ (solid line); 0.4 (dotted line); 0.6 (small-dashed line); 0.8 (dashed line); 1.0 (dot-dashed line.)